DOI 10.4430/bgo00435

Geophysical analysis using high-resolution aeromagnetic data of Jbel Ougnat, the Moroccan eastern Anti-Atlas: insights into geological structures and tectonic events

S. Sassioui[1], A. Aarab[1], K. Benyas[1], A. Idrissi[2], A. lakhloufi[1], O. Saidi[3], S. Courba[4] and A. Larabi[1]

[1] *Laboratory of Analysis and Modelling of Water and Natural Resources, Mohammadia School of Engineers, Mohammed V University, Rabat, Morocco*
[2] *Department of Earth Sciences, Faculty of Sciences, Mohamed V University, Rabat, Morocco*
[3] *Applied Geology Laboratory, Department of Geosciences, Faculty of Science and Techniques Errachidia, Moulay Ismail University, Meknes, Morocco*
[4] *Laboratory of Geosciences, Water and Environment, Department of Geology, Faculty of Sciences, Mohammed V University, Rabat, Morocco*

(Received: 19 April 2023; accepted: 6 October 2023; published online: 30 November 2023)

ABSTRACT Jbel Ougnat is the eastern extension of the eastern belt of the Anti-Atlas. This article focuses on a geophysical study using high-resolution aeromagnetic data covering the Jbel Ougnat area. These data were first filtered using several geophysical processing methods: reduction to the pole, horizontal gradient (*HG*), and Euler deconvolution (ED). They were, then, analysed and interpreted in the light of the geological background. The *HG* is used to detect magnetic lineaments, whereas the ED is used to estimate the location and depth of magnetic sources. The results obtained were compared with the geological maps and field survey data. The orientations of the lineaments, extracted from the *HG* map, are mainly trending NE-SW and NNW-SSE to N-S and NW-SE. The fieldwork helped to identify the mineralised features of these lineaments. The combination of these results with the depth values obtained from Euler solutions shows that these orientations are associated with several tectonic events, recorded by the area during its entire geological history.

Key words: Jbel Ougnat, eastern Anti-Atlas, geophysical study, aeromagnetic data, magnetic lineaments.

1. Introduction

The exposures of the Pan-African belt in Morocco are primarily characterised by the presence of Precambrian basement rocks located within a folded Palaeozoic belt of the Anti-Atlas, with NE-SW orientation as shown in Fig. 1A (Gasquet *et al*., 2008). These outcrop areas hold significant importance, as they serve both as a key to deciphering successive orogenic events and metallogenic provinces of the country. The Ougnat Massif is situated in the easternmost part of the Moroccan Anti-Atlas (Fig. 1B), which formed during the Pan-African orogeny (Ennih and Liégeois, 2001).

Geophysical techniques, including aeromagnetic, electric, and gravimetric, are increasingly used in structural mapping and mining prospecting. Magnetic surveys, for example, measure variations in the Earth's magnetic field to detect changes in the geological composition and

subsurface structure. This technique has proven to be valuable in mineral exploration, as it employs various approaches and algorithms to pinpoint the presence of minerals or deposits. Additionally, filters applied to aeromagnetic data, such as the horizontal gradient (*HG*) and Euler deconvolution (ED), enable the identification of geological structures like faults, lithological contacts, and dikes. The magnetic method, combined with the filters employed in this research, plays a role of utmost importance in refining the search for metallic and non-metallic mineral deposits and addressing geological challenges, thus rendering it indispensable in the field of Earth sciences. The effectiveness of this method in mineral exploration has been demonstrated in numerous studies conducted by researchers (e.g. Abdelrahman *et al*., 2003; Bouiflane *et al*., 2017; Essa and Elhussein, 2019; Rezouki *et al*., 2020; Benyas *et al*., 2021, 2022; Essa *et al*., 2021, 2023; Idrissi *et al*., 2021, 2022; Mehanee *et al*., 2021; Biswas *et al*., 2022; Mohamed *et al*., 2022; Tazi *et al*., 2022).

The study area has been subjected to several analyses and studies, among which structural, lithostratigraphic, and mineralogical, by numerous authors (e.g. Abia *et al*., 2003; Gasquet *et al*., 2005; Raddi *et al*., 2007; Baidder *et al*., 2008, 2016; Essalhi *et al*., 2017; Michard *et al*., 2017; Hejja *et al*., 2020; Aabi *et al*., 2021, 2022; Sassioui *et al*., 2022; Courba *et al*., 2023; Samaoui *et al*., 2023). However, none of the previous works studied the deep structures of the area using geophysical methods. Therefore, the present work shows and discusses the results of the mapping of the subsurface magnetic lineaments, and the identification of their depths, to fully understand the structural and geological framework of this area.

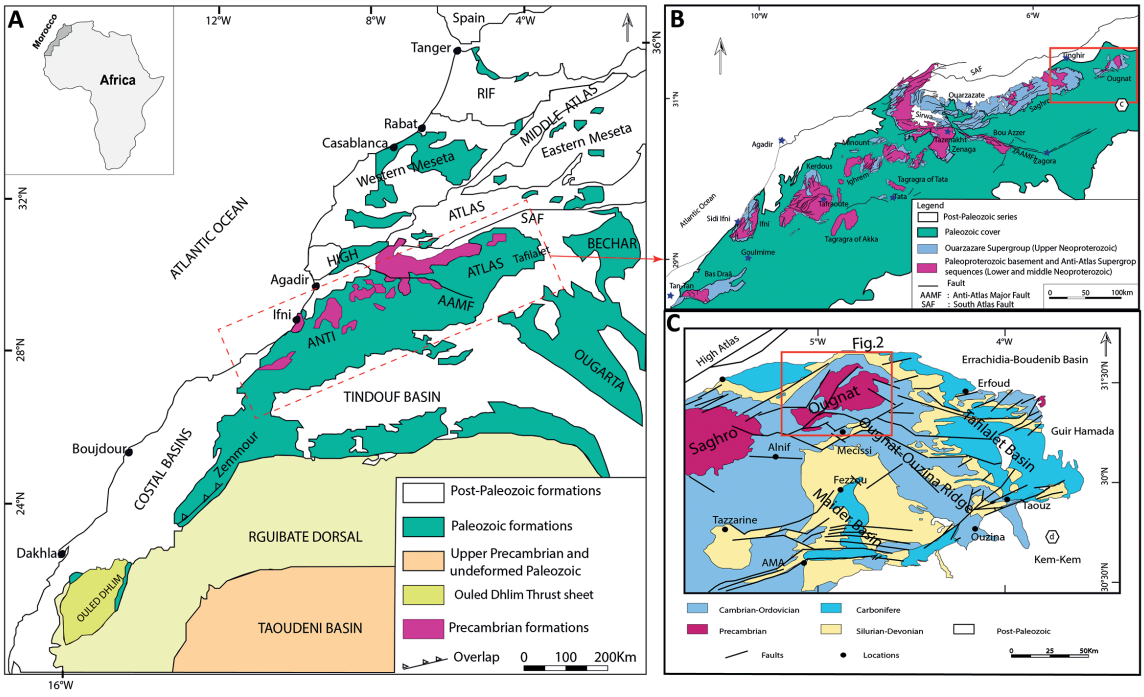

Fig. 1 - Geological location of the Ougnat Massif: A) map of geological Moroccan domains; B) Anti-Atlas geological map showing all Precambrian inliers surrounded by Palaeozoic rocks, adapted from a 1:1,000,000-scale geological map of Morocco (Geologic Service of Morocco, 1985); C) geological map of eastern Anti-Atlas (Michard *et al*., 2008; Baidder *et al*., 2016; Saidi *et al*., 2020), with the red rectangle in panel C indicating the study area.

2. Geological setting

The Ougnat Massif, the eastern part of the eastern Anti-Atlas, is mainly composed of two inliers: Saghro and Ougnat (Fig. 1C). It is characterised by a Precambrian basement formed during the Pan-African orogeny and, then, transformed into an in-extension-metacratonic domain throughout the end of the Neoproterozoic (Ennih and Liégeois, 2001; Gasquet *et al*., 2005). During the Palaeozoic, the study area recorded the imprint of several transgressions, ranging from the Middle Cambrian to the Lower Carboniferous period. The result of this transgression is the deposition of Palaeozoic sedimentary formations that outcrop around the Neoproterozoic basement (Hollard, 1974; Wendt, 1985). The sedimentary series were subjected to a compressive deformation during the Hercynian orogeny, which transformed these series into a SE-trending folded ridge [the Ougnat-Ouzina ridge (Hollard, 1974; Wendt, 1985; Baidder *et al*., 2008)].

The stratigraphy of Jbel Ougnat (Fig. 2) is composed of Neoproterozoic folded metasedimentary formations dated by U-Pb detrital zircon (Abati *et al*., 2010), that suggests a maximum age of 610-620 Myr for the Saghro Group sediments. The dating also shows that the Saghro Group was intruded recently by Mellab granitoid dated 547 ±26 Myr. The Ougnat anticlinal structure presents a complex assemblage of rocks, and a multiphase geological history. To identify the stratigraphy, the formations of the study area have been divided into three domains.

The Neoproterozoic volcanic-sedimentary basement (the Saghro Group) consists of deformed, schistose and metamorphosed quartzite schists and sandstones (Lécolle *et al*., 1991, 2003). These terrains outcrop in the central part of the massif, where granitoids have also been found in the form of two facies: quartzite diorites and garnet-granites (Marini and Ouguir, 1990). The setting of these two granitoids is synchronous (El Baghdadi *et al*., 2001).

The terminal Neoproterozoic volcanic-sedimentary formation (the Ouarzazate Group) is composed of a sequence of brecciated rocks, sandstones, and volcanic rocks (rhyolites, andesites, and ignimbrites) with intercalations of tuffs or eruptive breccias (Ennih and Liégeois, 2001; Thomas *et al*., 2002; Álvaro *et al*., 2014).

The Ouarzazate Group deposition was followed by the deposition of a Palaeozoic cover of significant unconformity. The Cambrian series contains the internal Feijas and Tabanit sandstone formations formed by paradoxides shales and sandstones, respectively (Destombes and Hollard, 1988). The Cambrian deposits are intercalated by alkaline basaltic formations and crowned by the rest of the Palaeozoic series (4 km thick), ranging from the Ordovician to the Lower Carboniferous, to the south and east of Jbel Ougnat (Raddi *et al*., 2007).

From a structural point of view, Ougnat, like all the Precambrian massifs of the Anti-Atlas, records several local and regional tectonic events. Two phases of deformation characterise the Pan-African orogeny: the major phase, B1, and the ultimate phase, B2 (Leblanc and Lancelot, 1980). The major phase, B1, corresponds to a phase of compressive deformation accompanied by a facies metamorphism. It is also characterised by isoclinal folds that extend southwards, and mainly affect the upper Proterozoic basement. The B1 phase has been attributed to the abduction of part of the oceanic crust on the NE edge of the West African Craton (WAC) (Leblanc and Lancelot, 1980). In contrast, the second phase, B2, has been described as an ultimate phase materialised by brittle deformation in the absence of metamorphism (Clauer and Leblanc, 1977). During the B2 phase, a collision was generated between the mobile lands, eastern Anti-Atlas and stable WAC (Leblanc and Lancelot, 1980).

The Hercynian orogeny is manifested by kilometric folds, trending NNE-SSW in the western Anti-Atlas, and E-W in the eastern and central Anti-Atlas. Metamorphism is absent or of low intensity (Raddi *et al*., 2007; Soulaimani *et al*., 2014).

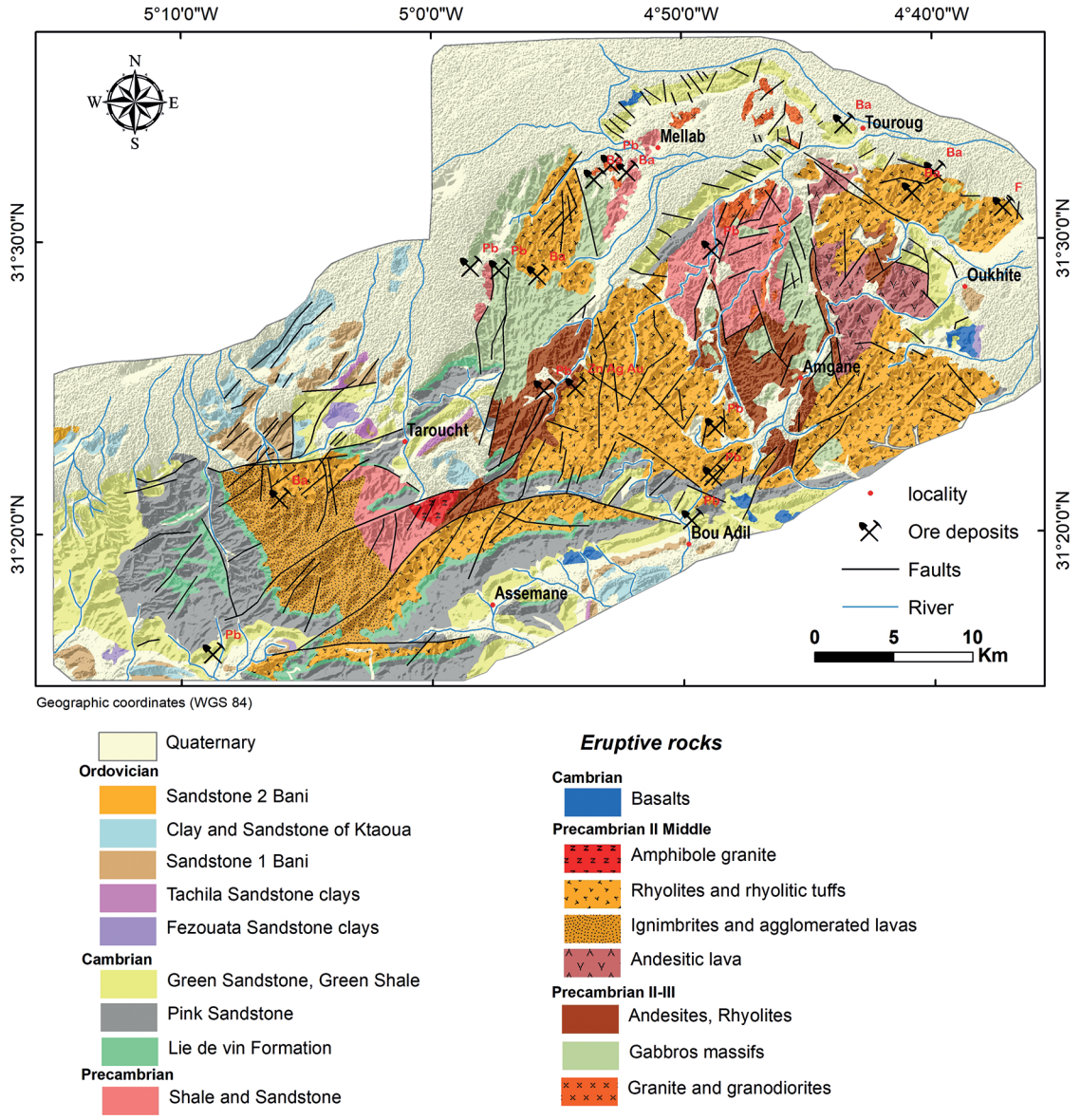

Fig. 2 - Geological map of Jbel Ougnat (Destombes and Hollard, 1988).

3. Data and methods

3.1. Aeromagnetic data

The compilation of the aeromagnetic data of the study area is based on the 1:50,000-scale maps (five maps: Bou Adil, Oukhit, Goulmima, Taroucht, and Touroug) provided by the Ministry of Energetic Transition and Sustainable Development. The geophysical survey was carried out between November 1998 and May 1999, with the aid of the Eurocopter AS35083, and AS35082 helicopters. At a height of 60 m above ground level, the magnetometer elevation was 30 m above ground level. The direction of the flight lines was 315°, 30°, and 15°, and the mean distance

between them was approximately 500 m. The tie lines for the crossover adjustment of the data were also flown at 45°, 120°, and 105° directions, with a mean distance of 4,000 and 8,000 m.

The total magnetic field data were recorded using a Scintrex CS2 magnetometer. After verification, the data underwent several corrections: denoising, closing errors, diurnal variation, and, for certain data sets and where needed, a threshold micro levelling treatment of 2 nT. The International Geomagnetic Field of Reference of the total area corrected has been extracted. The residual magnetic field values obtained have been interpolated using a 125-metre square mesh grid.

3.2 Field data

The field survey aimed to verify the lineaments found, by using geophysical processing, and to confirm whether they were mineralised or not. Therefore, we carried out several field surveys in the study area and oriented the examination, using the outcomes of the structural map generated through geophysical processing. The strategy was to verify most of the lineaments to confirm whether they coincided with the structural features, and, then, check for the presence of mineralisation.

3.3 Methods

In order to filter and use the aeromagnetic data, the process below has been followed. The values of the residual magnetic field contours were digitised with the flight lines and tie lines at the intersection point with ArcGIS software (Fig. 3), and converted to an Oasis Montaj regular mesh grid (Geosoft Inc., 2007).

With the mapping features of the Oasis Montaj program (Geosoft Inc., 2007), we created the residual magnetic field map using the database generated from these operations. The same software treated the residual map using several mathematical techniques.

The reduction to the pole (RTP) is used to eliminate the anomaly distortion caused by the tilt of the Earth's magnetic field, and to obtain anomalies whose maximum is centred on the magnetic sources (Blakely and Simpson, 1986). This is a basic feature of magnetic data processing

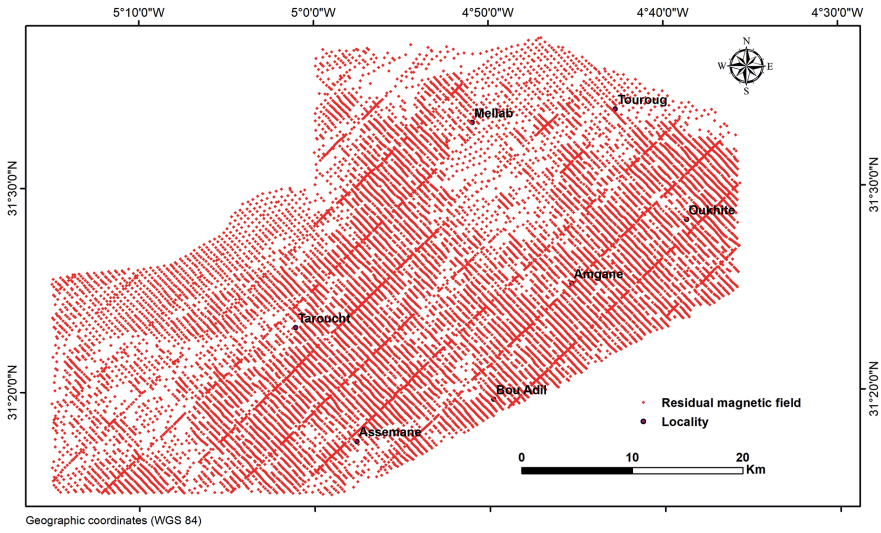

Fig. 3 - Representation of the data points used.

techniques. Due to the bipolarity of the magnetic field, the anomalies appear in a two-lobe format, which complicates their interpretation. The application of the RTP helps delineate the source of the magnetic anomalies, and, for this reason, the RTP is the first step in treating the magnetic data (Baranov, 1957; Baranov and Naudy, 1964).

The RTP map is fundamental for the processing workflow, as it will be used for the rest of the mathematical operations, including the *HG* and ED.

The *HG*, widely used by several authors (e.g. Cordell, 1979; Amiri *et al*., 2011; Azaiez *et al*., 2011; Gabtni *et al*., 2013; Dufréchou *et al*., 2014; Bba *et al*., 2019; Idrissi *et al*., 2022), is an effective source edge detection method used in structural mapping. In the present paper, the *HG* has been applied to reveal and detect linear structures that can be distinguished by abrupt changes in the magnetic field (Blakely and Simpson, 1986). The structures identified by this process can be described as geological contacts or subsurface faults.

The *HG* equation, developed by Cordell and Grauch (1985), can be expressed as follows:

$$HG(x,y) = \sqrt{(\frac{dT}{dx})^2 + (\frac{dT}{dy})^2} \quad (1)$$

where *T* is the total field reduced to the pole, and $\frac{dT}{dx}$ and $\frac{dT}{dy}$ are the first horizontal derivatives following *x* and *y*, respectively.

Furthermore, using the corresponding structural index (*SI*), the ED equation enables the detection and defining of the causative magnetic bodies, dykes, geological contacts, cylinders, and spheres (Reid *et al*., 1990). We highlighted the depth of magnetic faults with an *SI* equal to zero (Table 1), typically used to indicate large-scale faults (Harrouchi *et al*., 2016) and, as a result, create a magnetic lineament map of the study area. Thompson (1982) demonstrated that the Euler equation could be expressed (Table 2) as:

$$N(B-T) = \frac{(x-x0)\partial T}{\partial x} + \frac{(y-y0)\partial T}{\partial y} + \frac{(z-z0)\partial T}{\partial z}. \quad (2)$$

Table 1 - *N* values by source geometry (Reid *et al.*, 1990).

Geometric source	***N* (magnetism)**
Sphere	3
Vertical cylinder	2
Cylinder horizontal	2
Dyke / Sill	1
Contact	0

Table 2 - Terms of the ED equation.

Equation terms	**Significance**
x_0, y_0, z_0	Position of the magnetic sources
x, *y*, *z*	Observation point position
T	Total field detected at (*x*, *y*, *z*)
B	Regional value of the total field
N	Homogeneity degree often referred to as the *SI*, which characterises the type of source

4. Results

4.1. Residual field map

The examination of the residual map (Fig. 4) shows several anomaly types based on different shapes, sizes, and intensity values that vary between -300 and 500 nT.

However, the anomalies are generally asymmetric, consisting of two lobes (a positive lobe, coloured in red, and a negative lobe, coloured in blue). This geometry is related to the bipolarity of the Earth's magnetic field, making the interpretation of the anomalies difficult. For a better interpretation of the anomalies, the residual field map has been pole-reduced by introducing the RTP transformation.

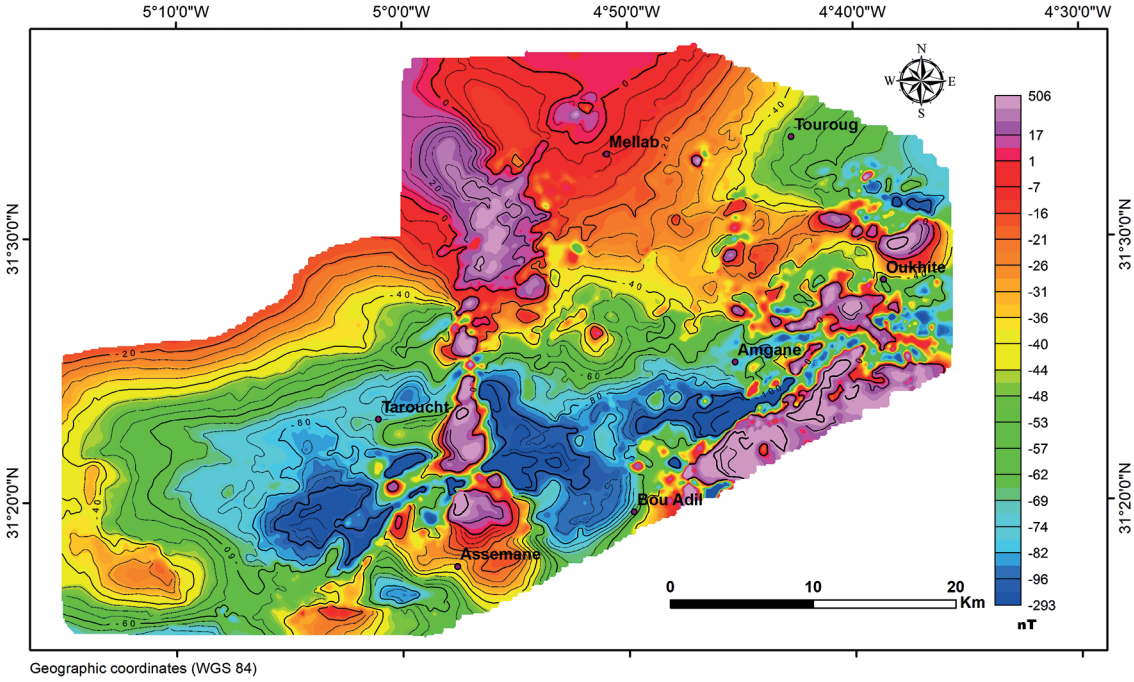

Fig. 4 - Residual magnetic field map of Jbel Ougnat.

4.2. Reduction to the pole (RTP) map

As mentioned, RTP processing has been applied to the residual anomaly map (inclination = 42.8°, declination = -3.4°). The first observation deduced from the RTP map (Fig. 5) is the displacement of the anomalies towards the north, as well as the increase of the magnetic field intensity values (the intensities vary between -380 and 600 nT instead of -300 and 500 nT). To facilitate the description, and subsequent interpretation of our results, the RTP map of the study area has been subdivided into six major areas based on the features of their anomalies.

The A Area, located in the centre of the map, presents a linear magnetic signature trending N-S, with positive intensity values of 200 nT. This anomaly coincides with the outcropping magmatic rocks, massive gabbros, andesites, and lower Proterozoic amphibole granites (PII-PII) (Fig. 2). These outcrops are situated along major N-S-trending faults.

The B Area, also located in the centre of the map, presents a large negative anomaly, 15 km long and 10 km wide, elongated according to an N-S to NNE-SSW direction. The intensity values of the B Area vary between -100 and -250 nT. According to the geological map of Ougnat (Fig. 2), the anomaly corresponds to the terminal Neoproterozoic rhyolites and tuffs.

The C Area is formed of two elongated negative anomalies trending NNE-SSW to NE-SW. The larger anomaly is 8 km long, with an intensity of -150 nT, while, in comparison, the smaller one is less important in intensity and size. These two anomalies correspond to Palaeozoic sedimentary terrains.

The D Area shows a very active magnetic field, dominated by positive anomalies of great intensities that reach 300 nT. The anomalies are elongated along two main directions, N-S and NE-SW. Based on the geological map (Fig. 2), these anomalies coincide with terminal Neoproterozoic magmatic formations such as andesitic lavas, andesites, and rhyolites. In the southern part of the D Area (east of the Bou Adil village, see Fig. 5), two negative anomalies of elliptical shape and intensity value of -200 nT have been observed. These correspond to Cambrian basalts.

The E Area is located to the west of the map (Fig. 2); the anomalous sources are allogenic, mainly trending N-S and NE-SW, with negative values ranging from 0 to -60 nT. They correspond to terminal Neoproterozoic ignimbrites and rhyolites.

The F Area is located between the two villages of Assemam and Taroucht, and includes small-sized anomalies. The first type of anomaly, elongated to the NE-SW, with intensity values of -10 nT, is located above granitic terrains. The second is elliptically shaped with intensity values of -100 nT. These areas are located above the terminal Neoproterozoic andesites.

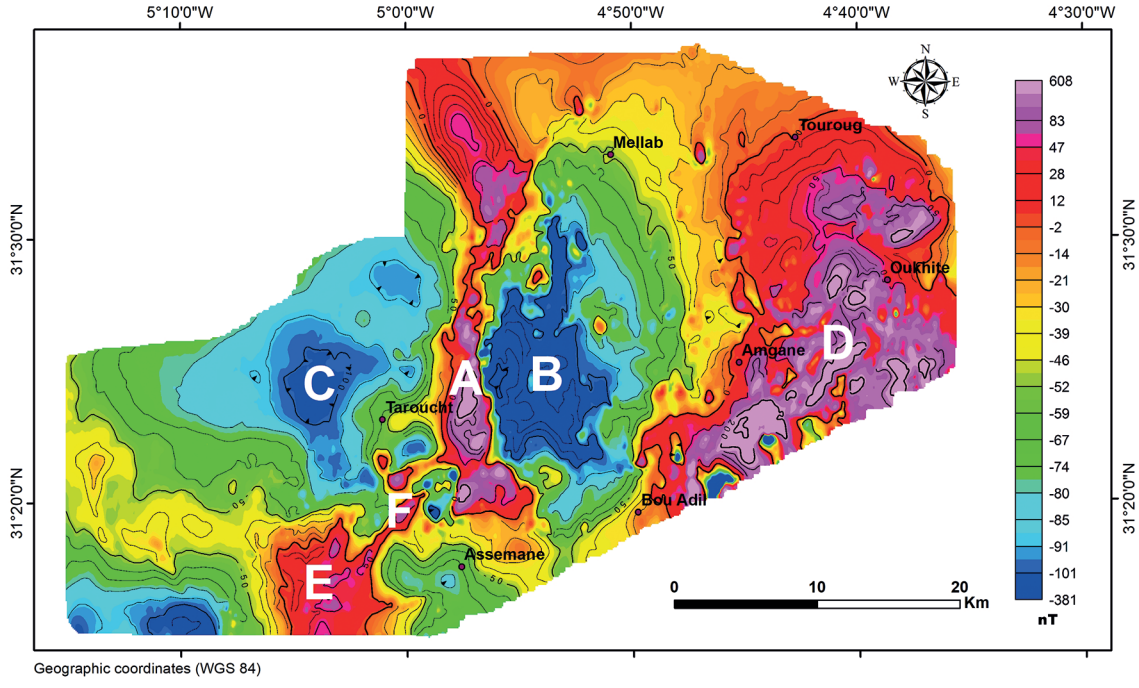

Fig. 5 - RTP map of Jbel Ougnat.

4.3. Horizontal gradient (HG) map

The *HG* is a highly effective filter in identifying linear magnetic sources, such as faults, lithologic contacts, and dykes, based on sudden changes in intensity. The *HG* map of the study area (Fig. 6) shows a set of magnetic lineaments of different directions, which were manually digitised according to the magnetic signal contrast.

The NE-SW-trending lineaments are the most dominant, and are found almost all over the study area, with an ascendency in the eastern and northern part of the map.

The N-S-trending system is located in the centre, with considerable lengths that reach from 10 to 15 km.

The lineaments trending NW-SE are generally situated in the eastern part of the Ougnat area. The E-W trending set is less represented on the map but is characterised by large extended lineaments located in the south-western part of the map.

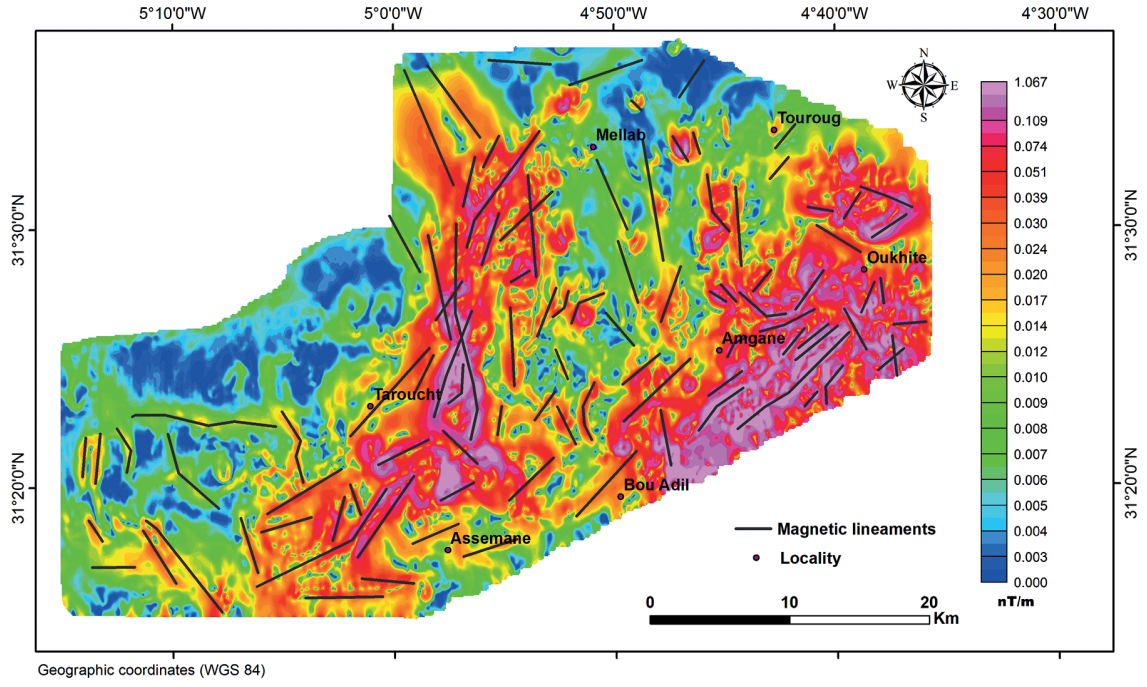

Fig. 6 - *HG* map.

4.4. Euler deconvolution (ED)

The ED technique has emerged as a highly effective and widely used method for interpreting and analysing potential field data. Its primary objective is to accurately estimate the location and depth of abnormal sources within the surveyed area, based on the *SI*. This technique has proven to be particularly valuable in geophysical studies, as it provides insights into subsurface structures and geological features. In our specific study, we focused on analysing the RTP aeromagnetic data collected at the Ougnat Massif. The main objective of this research was to estimate the depths of the linear features, known as lineaments, found in the study area. To ensure accurate results, a *SI* = 0 was selected, as such value is recommended for this type of investigation.

The depths of the detected lineaments varied between 500 and 2500 m, as illustrated in Fig. 7. This range indicates significant subsurface geological variations and highlights the potential presence of important geological structures at different depths. Understanding the depths of these lineaments is crucial for gaining insights into the geological history and potential resources within the Ougnat Massif.

The findings of the study further support the usefulness and relevance of the ED technique in geophysical analyses. By providing accurate estimations of depth, this technique enhances our understanding of the subsurface and facilitates geological interpretation. The results obtained provide valuable information for future exploration and resource assessment efforts in the Ougnat Massif, and other similar geological settings.

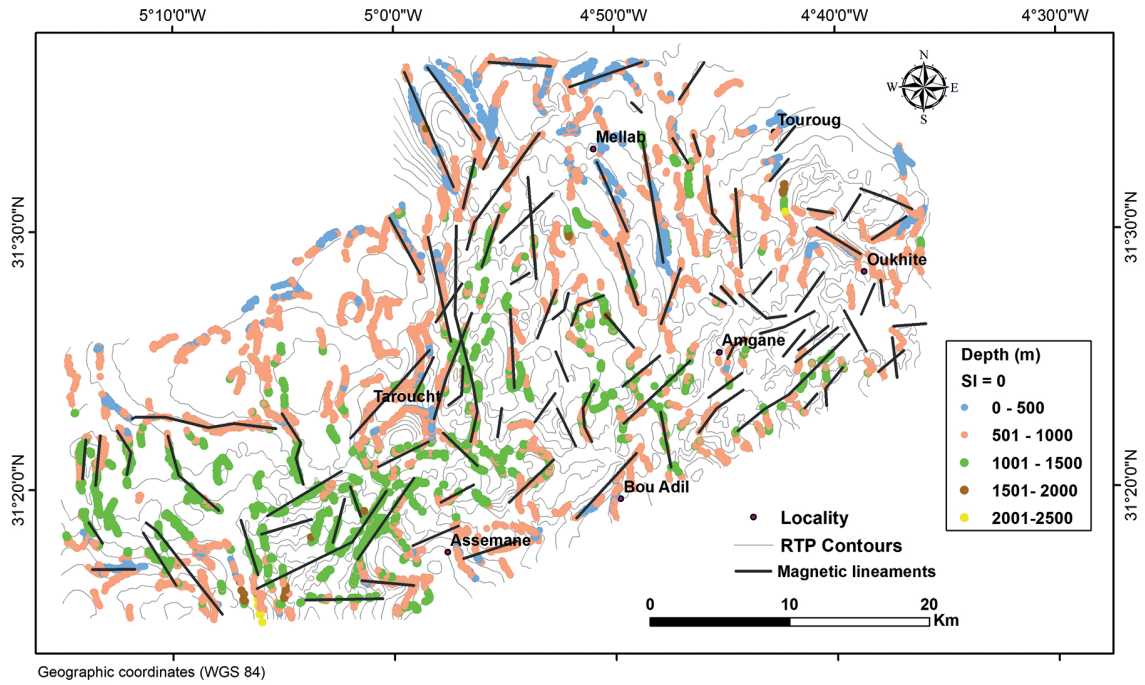

Fig. 7 - ED solution with the magnetic data (*SI* = 0, W = 8 × 8 km^2, *T* = 12%).

5. Discussion

The analysis and interpretation of the results obtained from the geophysical processing (RTP, *HG*, ED) are interpreted in the light of previous works such as Raddi *et al.* (2007), Baidder *et al.* (2008), Soulaimani and Burkhard (2008), Soulaimani *et al.* (2014), Michard *et al.* (2017), and Aabi *et al.* (2022). The results obtained from *HG* were compared with the data derived from the geological map of the study area (Fig. 8) by Destombes and Hollard (1988). This comparison revealed the alignment of geophysical lineaments with the previously mapped faults in the study area, thus indicating their compatibility.

The main directions found by the geophysical processing also showed a distribution of lineaments from N0° to N140°, with a predominance of the NE-SW direction. These directional families are interpreted as follows:

- lineaments of the NE-SW trending family are the most abundant in the area and exceed 1,000 m. In previous works, this direction of lineaments is related to the NW-SE directional compressive regime of the Pan-African orogeny that affected the Ougnat, which was reactivated as a reverse fault during the latest Variscan and Alpine tectonic events (Soulaimani and Burkhard, 2008; Álvaro *et al*., 2014; Soulaimani *et al*., 2014);
- lineaments of the NNW-SSE to N-S trending family are located in the centre of the Ougnat Massif and present kilometric lengths. Euler solutions show that they have significant depths of more than 1,000 m. This orientation correlates with the directions of ancient Pan-African fault systems;
- lineaments of the NW-SE trending family are represented having limited lengths, and shallow depths of <500 m. They are generally located in the Palaeozoic cover, which is explained by the fact that they are related to recent tectonic events (Gouiza *et al*., 2017).

The results obtained through the application of the ED technique were highly promising. There was a remarkable correlation between the Euler solutions and the magnetic lineaments derived from *HG* filter.

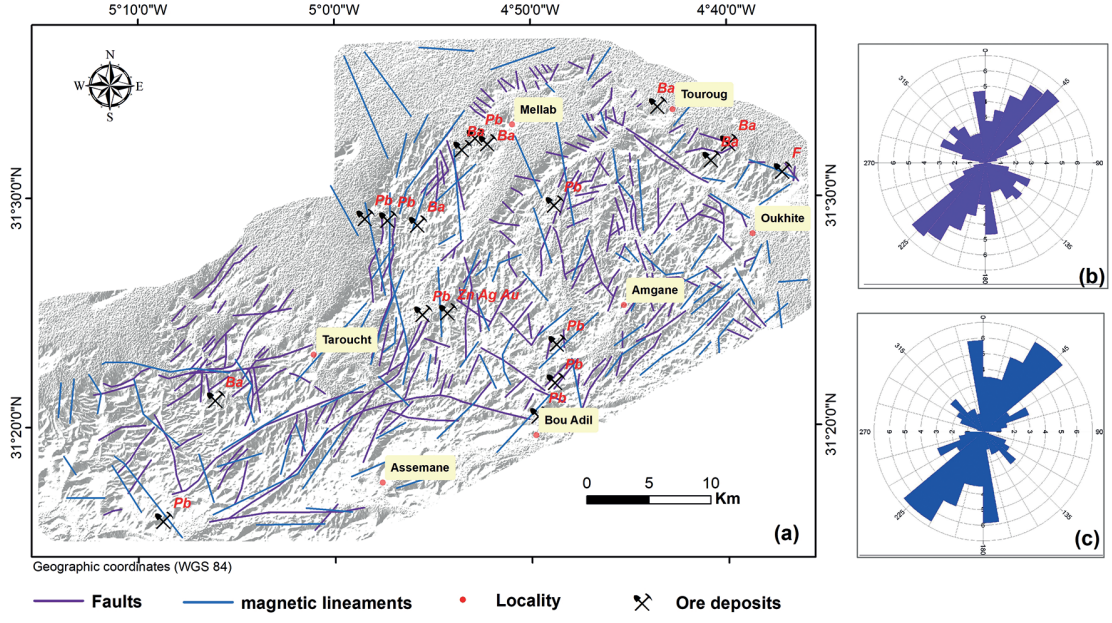

Fig. 8: - Structural map of Ougnat (a), directional rose of faults (b), and directional rose of magnetic lineaments (c).

To validate the results obtained from the geophysical processing, we compared the synthetic map gathering the different lineaments (Fig. 8a) with the faults digitised from the geological maps. The comparison outcomes showed that the geophysical lineaments coincided with the major faults of the study area (Fig. 8a). After field verification, these lineaments were found to correspond to both unmineralised tectonic fractures (Figs. 9A to 9C) and mineralised veins (Figs. 10D to 10H, and 11).

Furthermore, the network, newly generated from the geophysical treatments together with field observation, allows the identification of several new faults never mapped before in

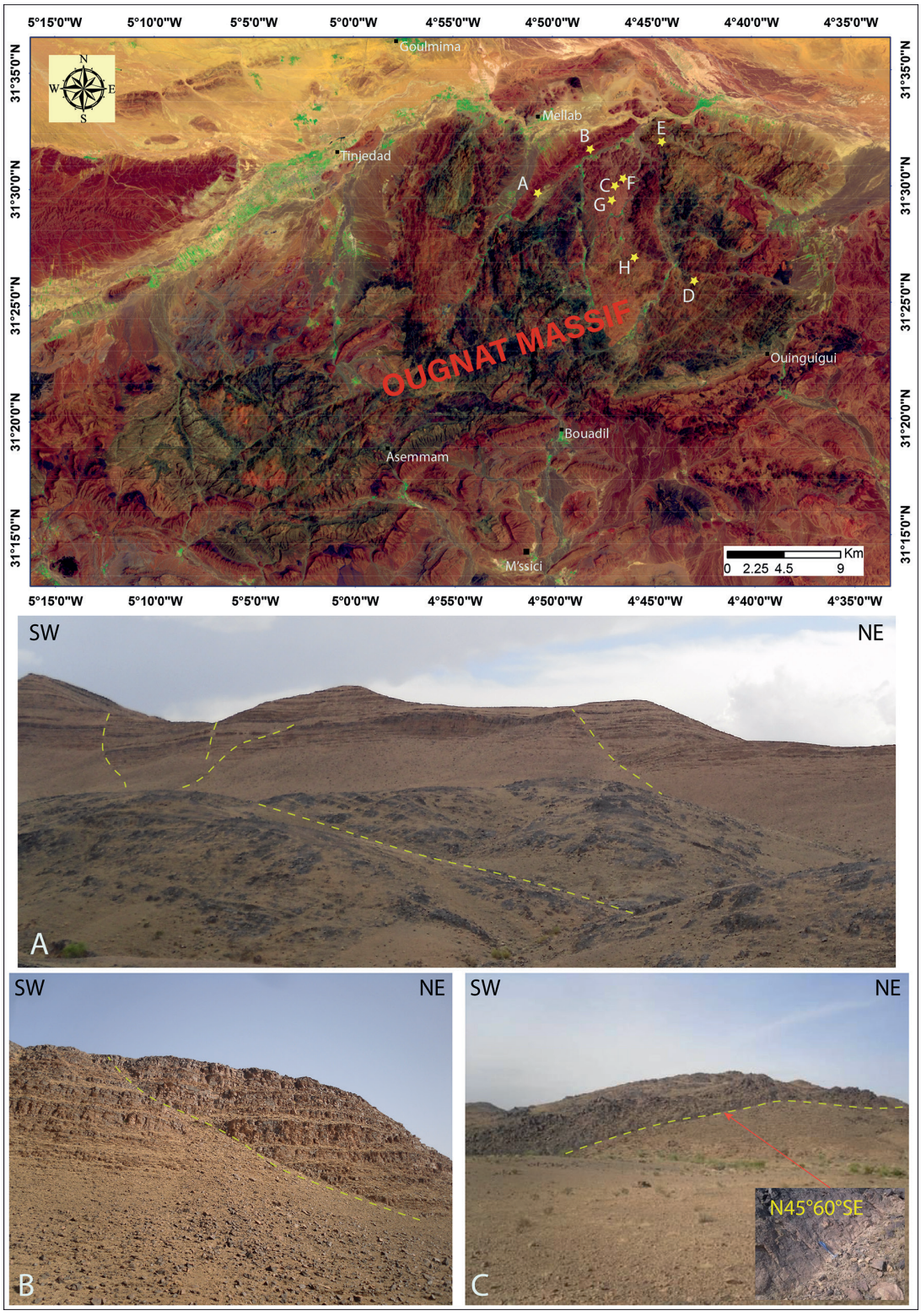

Fig. 9 - Landsat image extract showing the location of the different lineament validation points in the field, with panels A, B, and C showing photographic illustrations of a set of faults surveyed in the field.

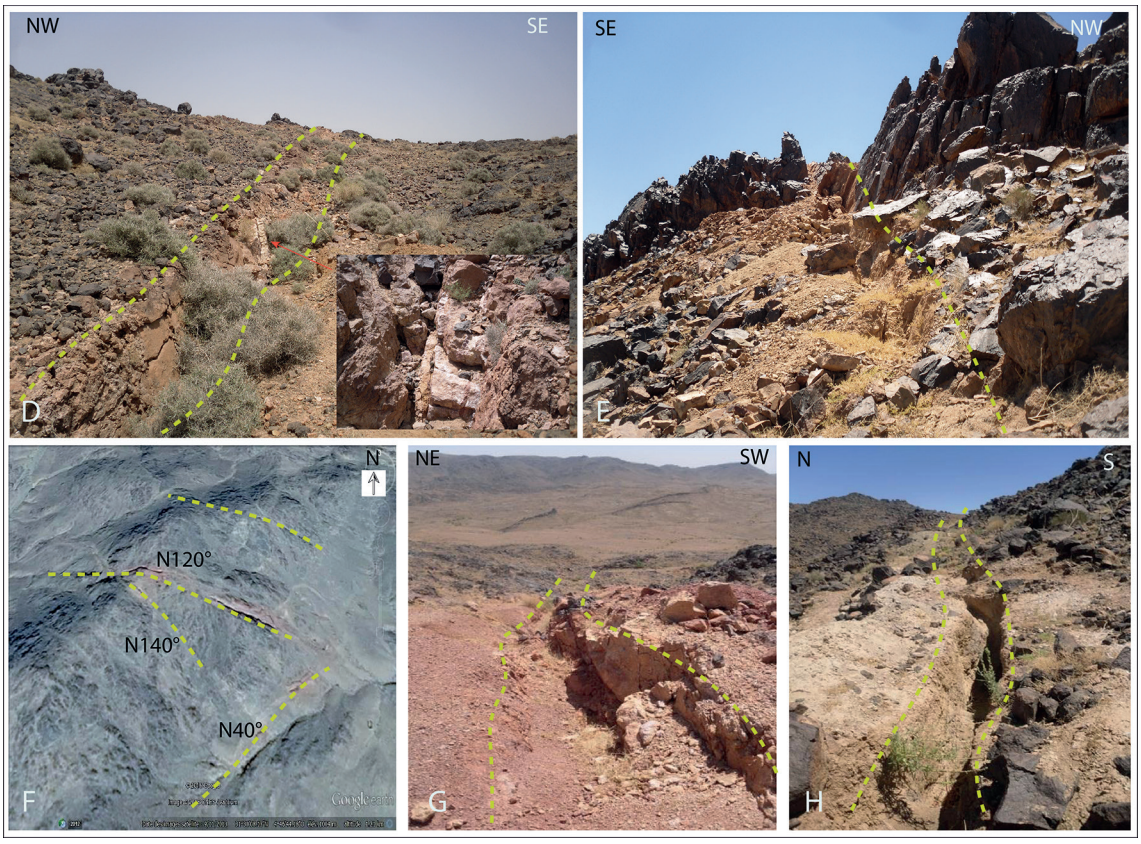

Fig. 10 - Photographs of mineralised structures (barite mining trenches) surveyed in the field with marking of the lineaments extracted from the geophysical treatments (see the location of pictures in panels D to H in Fig. 9).

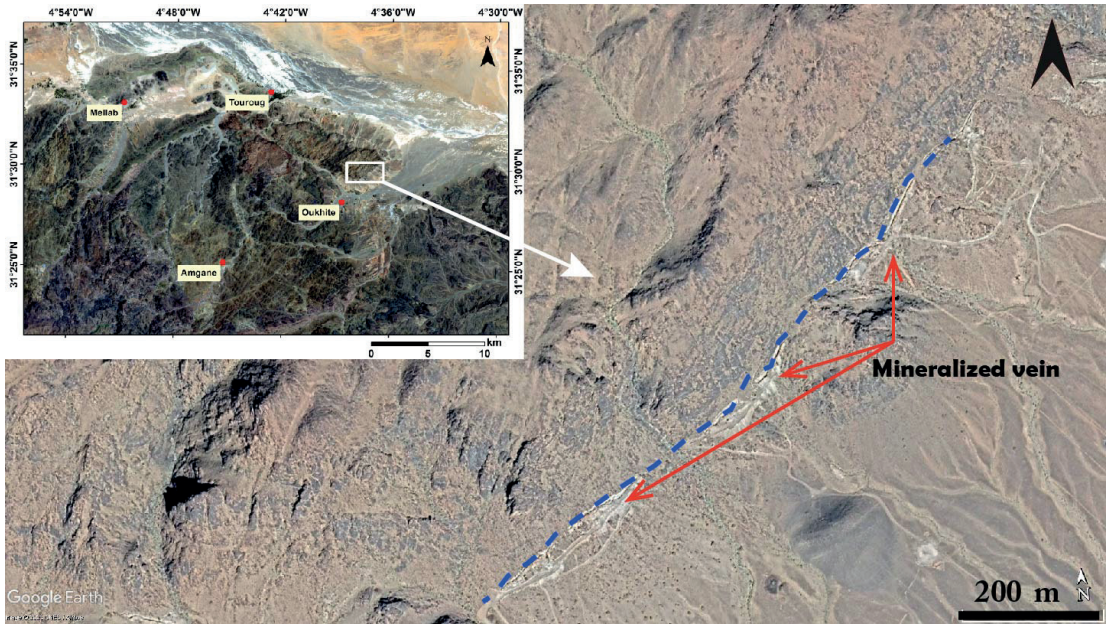

Fig. 11 - Barite vein (Google Earth image).

geological maps. By comparing the rose diagram of the geophysical lineaments with the rose diagram of the digitised and mapped fractures, a notable similarity in the main orientation and frequency (Figs. 8b and 8c) was observed. This approach confirms the faults already recognised by previous studies, and exposes the continuities of some major faults, resulting in a very useful outcome for the structural interpretation of the study area (Figs. 9A to 9C).

Moreover, the field observation indicates that the areas with a high lineament density constitute a preferred space for the circulation of hydrothermal fluids and deposition of mineralisation. Based on this logic, lineament density provides information on the influence that brittle tectonics have on the distribution of mineralised veins. Mineralisation in this region occurs in numerous veins of variable lengths, which can reach more than 1,000 m (Figs. 10D to 10H, and 11). Given that most of the fractures are mineralised (which is also an interesting fact from an economic point of view), the structural map generated in this work can be a valuable basis for metallogenic research and mineral exploration in the Ougnat Massif.

6. Conclusions

Geophysical mapping methods provide valuable information for the study of the Earth's subsurface, with both advantages and disadvantages. Advantages include non-invasiveness, testing in difficult or contaminated areas, wide-area coverage, characterisation of large regions with fewer tests, and relative cost-effectiveness given the vast areas covered. Conversely, there are limitations, such as limited resolution requiring invasive techniques for detailed observations and necessary knowledge on site conditions and target parameters for tool applicability. These factors underline the importance of understanding and addressing the strengths and limitations of geophysical mapping methods in order to achieve accurate and efficient subsurface analyses.

This work aims to interpret high-resolution aeromagnetic data (on a 1:50,000 scale) of Jbel Ougnat. The geophysical processing results mainly describe the structural indicators of the study area.

The map of the RTP residual magnetic field enabled identifying anomalies of different shapes, sizes, and orientations, where most of the anomalous sources correspond to Neoproterozoic volcanic rocks (rhyolites, ignimbrites, andesites, etc.), according to field investigations and geological maps.

The map generated by the *HG* enabled us to highlight the magnetic lineaments in the subsurface together with their characteristics and correlate them with the regional geological context. In general, the main directions of the magnetic lineaments are NE-SW, NNE-SSW to N-S, and NW-SE. They correspond to the major directions of the tectonic events that structured Jbel Ougnat over time. Using the ED, each magnetic structure was matched to its depth. The shallower features are NW-SE trending, their depths are less than 500 m, and they are mainly located on the Palaeozoic cover. The lineaments trending NNW-SSE to N-S are situated in the centre of the Ougnat area, and their corresponding depths reach more than 1,000 m, with the deepest being the NE-SW trending lineaments.

As for mineralisation, the area involved is part of the Moroccan metallogenic province of the Anti-Atlas, which presents numerous mineralogical activities. The study carried out on this massif could lead us to believe that it may be considered as one of the best guides for a future mineralogical prospection.

REFERENCES

Aabi A., Baidder L., Hejja Y., Mohammed E.A., Bba N.-B. and Otmane K.; 2021: *The Cu-Pb-Zn-bearing veins of the Bou Skour deposit (eastern Anti-Atlas, Morocco): structural control and tectonic evolution.* C. R. Geosci., 353, 81-99, doi: 10.5802/crgeos.54.

Aabi A., Hejja Y., Bba A.N., Baidder L., Fekkak A., Bannari A. and Maacha L.; 2022: *Polyphase tectonics, fault kinematics and metallogenic implications at the fringe of a craton (Anti-Atlas, Morocco).* J. Afr. Earth Sci., 196, 104731, 20 pp., doi: 10.1016/j.jafrearsci.2022.104731.

Abati J., Aghzer A.M., Gerdes A. and Ennih N.; 2010: *Detrital zircon ages of Neoproterozoic sequences of the Moroccan Anti-Atlas belt.* Precambrian Res., 181, 115-128, doi: 10.1016/j.precamres.2010.05.018.

Abdelrahman E.M., El-Arby H.M., El-Arby T.M. and Essa K.S.; 2003: *A least-squares minimization approach to depth determination from magnetic data.* Pure Appl. Geophys., 160, 1259-1271, doi: 10.1007/s000240300005.

Abia E.H., Nachit H., Marignac C., Ibhi A. and Saadi S.A.; 2003: *The polymetallic Au-Ag-bearing veins of Bou Madine (Jbel Ougnat, eastern Anti-Atlas, Morocco): tectonic control and evolution of a Neoproterozoic epithermal deposit.* J. Afr. Earth Sci., 36, 251-271, doi: 10.1016/S0899-5362(03)00051-4.

Álvaro J.J., Benziane F., Thomas R., Walsh G.J. and Yazidi A.; 2014: *Neoproterozoic-Cambrian stratigraphic framework of the Anti-Atlas and Ouzellagh promontory (high Atlas), Morocco.* J. Afr. Earth Sci., 98, 19-33, doi: 10.1016/j.jafrearsci.2014.04.026.

Amiri A., Chaqui A., Hamdi Nasr I., Inoubli M.H., Ben Ayed N. and Tlig S.; 2011: *Role of preexisting faults in the geodynamic evolution of northern Tunisia, insights from gravity data from the Medjerda valley.* Tectonophys., 506, 1-10, doi: 10.1016/j.tecto.2011.03.004.

Azaiez H., Gabtni H., Bouyahya I., Tanfous D. and Bedir M.; 2011: *Lineaments extraction from gravity data by automatic lineament tracing method in Sidi Bouzid basin (central Tunisia): structural framework inference and hydrogeological implication.* Int. J. Geosci., 2, 373-383, doi: 10.4236/ijg.2011.23040.

Baidder L., Raddi Y., Tahiri M. and Michard A.; 2008: *Devonian extension of the Pan-African crust north of the West African craton, and its bearing on the Variscan foreland deformation: evidence from eastern Anti-Atlas (Morocco).* Geol. Soc., London, Spec. Publ., 297, 453-465, doi: 10.1144/SP297.21.

Baidder L., Michard A., Soulaimani A., Fekkak A., Eddebbi A., Rjimati E.-C. and Raddi Y.; 2016: *Fold interference pattern in thick-skinned tectonics; a case study from the external Variscan belt of eastern Anti-Atlas, Morocco.* J. Afr. Earth Sci., 119, 204-225, doi: 10.1016/j.jafrearsci.2016.04.003.

Baranov V.; 1957: *A new method for interpretation of aeromagnetic maps: pseudo-gravimetric anomalies*. Geophys., 22, 359-382, doi: 10.1190/1.1438369.

Baranov V. and Naudy H.; 1964: *Numerical calculation of the formula of reduction to the magnetic pole*. Geophys., 29, 67-79, doi: 10.1190/1.1439334.

Bba A.N., Boujamaoui M., Amiri A., Hejja Y., Rezouki I., Baidder L., Inoubli M.H., Manar A. and Jabour H.; 2019: *Structural modeling of the hidden parts of a Paleozoic belt: insights from gravity and aeromagnetic data (Tadla basin and Phosphates plateau, Morocco)*. J. Afr. Earth Sci., 151, 506-522, doi: 10.1016/j.jafrearsci.2018.09.007.

Benyas K., Aarab A., Qarbous A., Lakhloufi A., Manar A., Amar M., Idrissi A. and Elmimouni M.; 2021: *Iraqi geological journal exploiting aeromagnetic and gravity data interpretation to delineate massif deposits of Rehamna area (western Meseta-Morocco).* Iraqi Geol. J., 54, 13-28, doi: 10.46717/igj.54.2C.2Ms-2021-09-21.

Benyas K., Aarab A., Lakhloufi A., Qarbous A., Manar A., Amar M., Idrissi A. and El-Mimouni M.; 2022: *Contribution of the airborne magnetic field to the structural study of the Variscan granitoid of Rehamna, Morocco.* Iraqi Geol. J., 55, 21-39, doi: 10.46717/igj.55.1A.2Ms-2022-01-21.

Biswas A., Rao K. and Mondal T.S.; 2022: *Inverse modeling and uncertainty assessment of magnetic data from 2D thick dipping dyke and application for mineral exploration.* J. Appl. Geophys., 207, 104848, 13 pp., doi: 10.1016/j.jappgeo.2022.104848.

Blakely R.J. and Simpson R.W.; 1986: *Approximating edges of source bodies from magnetic or gravity anomalies*. Geophys., 51, 1494-1498, doi: 10.1190/1.1442197.

Bouiflane M., Manar A., Medina F., Youbi N. and Rimi A.; 2017: *Mapping and characterization from aeromagnetic data of the Foum Zguid dolerite Dyke (Anti-Atlas, Morocco) a member of the Central Atlantic Magmatic Province (CAMP).* Tectonophys., 708, 15-27, doi: 10.1016/j.tecto.2017.04.023.

Clauer N. and Leblanc M.; 1977: *Implications stratigraphiques d'une étude géochronologique Rb-Sr sur métasédiments précambriens de BouAzzer (Anti-Atlas, Maroc).* Notes Mém. Serv. Géol. Maroc, 38, 7-12.

Cordell L.; 1979: *Gravimetric expression of graben faulting in Santa Fe country and the Espanola basin, New Mexico.* In: Ingersoll R.V., Woodward L.A. and James H.L. (eds), 30th Annual Fall Field Conference Guidebook, Geological Society, Santa Fe Country, NM, USA, pp. 59-64, doi: 10.56577/FFC-30.

Cordell L. and Grauch V.J.S.; 1985: *Mapping basement magnetization zones from aeromagnetic data in the San Juan basin, New Mexico*. In: Hinze W.J. (ed), The utility of regional gravity and magnetic anomaly maps, Society of Exploration Geophysicists, Houston, TX, USA, pp. 181-197, doi: 10.1190/1.0931830346.ch16.

Courba S., Hahou Y., Achmani J., Ouallali A., El Amrani M., Boudad A., Idrissi A., Aafir Z., Sassioui S., Ousaid L., Ghadi T., Lamchaimech A. and Ben Driss M.A.; 2023: *Litho-structural and hydrothermal alteration mapping for mineral prospection in the Maider basin of Morocco based on remote sensing and field investigations.* Remote Sens. Appl.: Soc. Environ., 31, 100980, 20 pp., doi: 10.1016/j.rsase.2023.100980.

Destombes J. and Hollard H.; 1988: *Carte géologique du Maroc au 1:200 000, feuille Todgha-Ma'der.* Notes Mém. Serv. Géol. Maroc, 243, Rabat, Morocco.

Dufréchou G., Harris L.B. and Corriveau L.; 2014: *Tectonic reactivation of transverse basement structures in the Grenville orogen of SW Quebec, Canada: insights from gravity and aeromagnetic data.* Precambrian Res., 241, 61-84, doi: 10.1016/j.precamres.2013.11.014.

El Baghdadi M., El Boukhari A., Jouider A., Benyoucef A. and Nadem S.C.; 2001: *Typologie du zircon des granitoïdes de Bouskour et d'Ougnat (Saghro, Anti-Atlas, Maroc): comparaison et signification géodynamique Zircon typology of Bouskour and Ougnat granitoids (Saghro, Anti-Atlas, Morocco): comparison and geodynamic implication*, Pangea, 35/36, 5-26.

Ennih N. and Liégeois J.-P.; 2001: *The Moroccan Anti-Atlas: the West African craton passive margin with limited Pan-African activity. Implications for the northern limit of the craton.* Precambrian Res., 112, 289-302, doi: 10.1016/S0301-9268(01)00195-4.

Essa K.S. and Elhussein M.; 2019: *Magnetic interpretation utilizing a new inverse algorithm for assessing the parameters of buried inclined dike-like geological structure.* Acta Geophys., 67, 533-544, doi: 10.1007/s11600-019-00255-9.

Essa K.S., Mehanee S. and Elhussein M.; 2021: *Magnetic data profiles interpretation for mineralized buried structures identification applying the variance analysis method.* Pure Appl. Geophys., 178, 973-993, doi: 10.1007/s00024-020-02553-6.

Essa K.S., Abo-Ezz E.R., Géraud Y. and Diraison M.; 2023: *A successful inversion of magnetic anomalies related to 2D dyke-models by a particle swarm scheme.* J. Earth Syst. Sci., 132, 1-16, doi: 10.1007/s12040-023-02075-4.

Essalhi A., Essalhi M., Toummite A., Mostadi A. and Raddi Y.; 2017: *Mineralogical and textural arguments for a metasomatic origin of the Ougnat pyrophyllite, eastern Anti-Atlas, Morocco.* J. Mater. Environ. Sci., 8, 22-32.

Gabtni H., Jallouli C., Mickus K.L. and Turki M.M.; 2013: *Geodynamics of the southern Tethyan margin in Tunisia and Maghrebian domain: new constraints from integrated geophysical study*. Arabian J. Geosci., 6, 271-286, doi: 10.1007/s12517-011-0362-z.

Gasquet D., Levresse G., Cheilletz A., Azizi-Samir M.R. and Mouttaqi A.; 2005: *Contribution to a geodynamic reconstruction of the Anti-Atlas (Morocco) during Pan-African times with the emphasis on inversion tectonics and metallogenic activity at the Precambrian-Cambrian transition.* Precambrian Res., 140, 157-182, doi: 10.1016/j.precamres.2005.06.009.

Gasquet D., Ennih N., Liégeois J.-P., Soulaimani A. and Michard A.; 2008: *The Pan-African belt.* In: Michard A., Saddiqi O., Chalouan A. and de Lamotte D.F. (eds), Continental Evolution: the Geology of Morocco. Structure, stratigraphy, and tectonics of the Africa-Atlantic-Mediterranean Triple Junction, 1 ed., Springer, Berlin, Heidelberg, Germany, Lecture Notes in Earth Sciences, 116, pp. 33-64, doi: 10.1007/978-3-540-77076-3_2.

Geologic Service of Morocco; 1985: *Geological map of Morocco at 1:1 000 000*. Notes Memory, N 260, Rabat, Morocco.

Geosoft Inc.; 2007: *Oasis Montaj.* Toronto, ON, Canada, <www.geosoft.com/media/uploads/resources/brochures/OM_b_2008_10_web.pdf>.

Gouiza M., Charton R., Bertotti G., Andriessen P. and Storms J.E.A.; 2017: *Post-Variscan evolution of the Anti-Atlas belt of Morocco constrained from low-temperature geochronology.* Int. J. Earth Sci., 106, 593-616, doi: 10.1007/s00531-016-1325-0.

Harrouchi L., Hamoudi M., Bendaoud A. and Beguiret L.; 2016: *Application of 3D Euler deconvolution and improved tilt angle to the aeromagnetic data of In Ouzzal terrane, western Hoggar, Algeria.* Arabian J. Geosci., 9, 508, 11 pp., doi: 10.1007/s12517-016-2536-1.

Hejja Y., Baidder L., Ibouh H., Bba A.N., Soulaimani A., Gaouzi A. and Maacha L.; 2020: *Fractures distribution and basement-cover interaction in a polytectonic domain: a case study from the Saghro Massif (eastern Anti-Atlas, Morocco)*. J. Afr. Earth Sci., 162, 103694, 16 pp., doi: 10.1016/j.jafrearsci.2019.103694.

Hollard H.; 1974: *Recherches sur la stratigraphie des formations du Dévonien moyen, de l›Emsien supérieur au Frasnien, dans le sud du Tafilalt et dans le Maider (Anti-Atlas oriental,* Notes Mém. Serv. Géol. Maroc, 264, 7-68.

Idrissi A., Saadi M., Manar A., Astati Y., Harrouchi L. and Nacer J.E.; 2021: *Contribution of aeromagnetic cartography and lithostratigraphic studies to the identification of blind faults and the Cambrian deposits geometry in Jbel Saghro (eastern Anti-Atlas, Morocco).* Boll. Geof. Teor. Appl., 62, 101-118, doi: 10.4430/bgo0335.

Idrissi A., Saadi M., Astati Y., Harrouchi L., Nacer J.E., Bouayachi A. and Benyas K.; 2022: *Contribution of gravity anomalies interpretation to the geology of the Jbel Saghro (eastern Anti-Atlas, Morocco): implications for the impact of structural control on sedimentation distribution.* Bull. Geoph. Ocean., 63, 215-236, doi: 10.4430/bgo00381.

Leblanc M. and Lancelot J.R.; 1980: *Interprétation géodynamique du domaine pan-africain (Précambrien terminal) de l'Anti-Atlas (Maroc) à partir de données géologiques et géochronologiques.* Can. J. Earth Sci., 17, 142-155, doi: 10.1139/e80-012.

Lécolle M., Derré C. and Nerci K.; 1991: *The Proterozoic sulphide alteration pipe of Sidi Flah and its host series. New data for the geotectonic evolution of the Pan-African belt in the eastern Anti-Atlas (Morocco).* Ore Geol. Rev., 6, 501-536, doi: 10.1016/0169-1368(91)90045-9.

Lécolle M., Derré C. and Hadri M.; 2003: *Les protolites des altérites à pyrophyllite de l'Ougnat et leurs positions dans l'histoire du Protérozoïque: mise à jour des connaissances géologiques sur l'Anti-Atlas oriental.* Afr. Geosci. Rev., 10, 227-244.

Marini F. and Ouguir H.; 1990: *Un nouveau jalon dans l'histoire de la distension pré-panafricaine au Maroc: le Précambrien II des boutonnières du Jbel Saghro nord-oriental (Anti-Atlas, Maroc).* C.R. Acad. Sci., Ser. IIb: Mec., Phys., Chim., Astron., 310, 577-582.

Mehanee S., Essa K.S. and Diab Z.E.; 2021: *Magnetic data interpretation using a new R-parameter imaging method with application to mineral exploration.* Nat. Resour. Res., 30, 77-95, doi: 10.1007/s11053-020-09690-8.

Michard A., Hoepffner C., Soulaimani A. and Baidder L.; 2008: *The Variscan belt.* In: Michard A., Saddiqi O., Chalouan A. and de Lamotte D.F. (eds), Continental Evolution: the Geology of Morocco. Structure, stratigraphy, and tectonics of the Africa-Atlantic-Mediterranean Triple Junction, 1 ed., Springer, Berlin, Heidelberg, Germany, Lecture Notes in Earth Sciences, pp. 65-132, doi: 10.1007/978-3-540-77076-3_3.

Michard A., Soulaimani A., Ouanaimi H., Raddi Y., Aït Brahim L., Rjimati E.-C., Baidder L. and Saddiqi O.; 2017: *Saghro group in the Ougnat Massif (Morocco), an evidence for a continuous Cadomian basin along the northern West African craton.* C. R. Geosci, 349, 81-90, doi: 10.1016/j.crte.2017.01.001.

Mohamed A., Abdelrady M., Alshehri F., Mohammed M.A. and Abdelrady A.; 2022: *Detection of mineralization zones using aeromagnetic data.* Appl. Sci., 12, 9078, 16 pp., doi: 10.3390/app12189078.

Raddi Y., Baidder L., Tahiri M. and Michard A.; 2007: *Variscan deformation at the northern border of the West African craton, eastern Anti-Atlas, Morocco: compression of a mosaic of tilted blocks.* Bull. Soc. Géol. Fr., 178, 343-352, doi: 10.2113/gssgfbull.178.5.343.

Reid A.B., Allsop J.M., Granser H., Millett A.J. and Somerton I.W.; 1990: *Magnetic interpretation in three dimensions using Euler deconvolution.* Geophys., 55, 80-91, doi: 10.1190/1.1442774.

Rezouki I., Boujamaoui M., Hafid M., Bba A.N., Amiri A., Inoubli M.H., Manar A., Rouai M., Baidder L. and Asebriy L.; 2020: *Contribution of gravity and aeromagnetic data to the structural modeling of the hidden faults in Guercif basin, northeastern Morocco.* J. Afr. Earth Sci., 164, 103797, 19 pp., doi: 10.1016/j.jafrearsci.2020.103797.

Saidi O., Mhamdi H.S., Essalhi A. and Toummite A.; 2020: *Mapeo de redes de fracturas mediante imágenes Landsat-8 OLI en la zona minera de Jbel Tijekht en el Anti-Atlas oriental de Marruecos.* Estud. Geol., 76, e133, 18 pp., doi: 10.3989/egeol.43887.587.

Samaoui S., Aabi A., Nguidi M.A., Boushaba A., Belkasmi M., Baidder L., Bba A.N., Lamrani O., Taadid M. and Zehni A.; 2023: *Fault-controlled barite veins of the eastern Anti-Atlas (Ougnat, Morocco), a far-field effect of the central Atlantic opening? Structural analysis and metallogenic implications.* J. Afr. Earth Sci., 104970, 16 pp., doi: 10.1016/j.jafrearsci.2023.104970.

Sassioui S., Aarab A., Darbali M., Ouchbani A., Lakhloufi A., Hilali M.E. and Larabi A.; 2022: *Contribution to the mineralogical study using electrical tomography in Foum Tizza area, eastern Anti-Atlas, Morocco.* Iraqi Geol. J., 1-13, doi: 10.46717/igj.55.2D.1ms-2022-10-17.

Soulaimani A. and Burkhard M.; 2008: *The Anti-Atlas chain (Morocco): the southern margin of the Variscan belt along the edge of the West African craton.* Geol. Soc., London, Spec. Publ., 297, 433-452, doi: 10.1144/SP297.20.

Soulaimani A., Michard A., Ouanaimi H., Baidder L., Raddi Y., Saddiqi O. and Rjimati E.C.; 2014: *Late Ediacaran-Cambrian structures and their reactivation during the Variscan and Alpine cycles in the Anti-Atlas (Morocco).* J. Afr. Earth Sci., 98, 94-112, doi: 10.1016/j.jafrearsci.2014.04.025.

Tazi M.J., El Azzab D., Mohammed C., Jabrane O., Ouahzizi Y., Zahour R. and Amadou A.; 2022: *Identification of potential mineral exploration targets from the interpretation of aeromagnetic data covering the Sirwa region (central Anti-Atlas, Morocco).* Sci. Afr., 17, e01351, 13 pp., doi: 10.1016/j.sciaf.2022.e01351.

Thomas R.J., Chevallier L.P., Gresse P.G., Harmer R.E., Eglington B.M., Armstrong R.A., de Beer C.H., Martini J.E.J., de Kock G.S., Macey P.H. and Ingram B.A.; 2002: *Precambrian evolution of the Sirwa window, Anti-Atlas orogen, Morocco*. Precambrian Res., 118, 1-57, doi: 10.1016/S0301-9268(02)00075-X.

Thompson D.T.; 1982: *EULDPH: a new technique for making computer-assisted depth estimates from magnetic data.* Geophys., 47, 31-37, doi: 10.1190/1.1441278.

Wendt J.; 1985: *Disintegration of the continental margin of northwestern Gondwana: Late Devonian of the eastern Anti-Atlas (Morocco).* Geol., 13, 815-818, doi: 10.1130/0091-7613(1985)13<815:DOTCMO>2.0.CO;2.

Corresponding author: Slimane Sassioui
Mohammadia School of Engineers, Mohammed V University
Ibn Sina Street, PB 765, Rabat, Morocco
Phone: +212 606885485; e-mail: sassiouislimane@gmail.com